Journal of Magnetism and Magnetic Materials 321 (2009) 295–299

Contents lists available at ScienceDirect

Journal of Magnetism and Magnetic Materials

journal homepage: www.elsevier.com/locate/jmmm

Magnetic properties for the Mn_2GeTe_4 compound

M. Quintero [a,*], E. Quintero [a], D. Caldera [a], E. Moreno [a], M. Morocoima [a], P. Grima [a], D. Ferrer [a], N. Marchan [a], P. Bocaranda [a], G.E. Delgado [b], J.A. Henao [c], M.A. Macías [c], J.L. Pinto [c], C.A. Ponce [d]

[a] Departamento de Física, Facultad de Ciencias, Centro de Estudios de Semiconductores, Universidad de los Andes, Mérida 5101, Venezuela
[b] Laboratorio de Cristalografía, Departamento de Química, Facultad de Ciencias, Universidad de Los Andes, Mérida 5101, Venezuela
[c] Grupo de Investigación en Química Estructural (GIQUE), Centro de Investigación en Biomoléculas (CIBIMOL), Facultad de Ciencias, Escuela de Química, Universidad Industrial de Santander, Apartado aéreo 678, Bucaramanga, Colombia
[d] Facultad de Ciencias Exactas y Naturales y Agrimensura, Universidad Nacional del Nordeste, Corrientes 3400, Argentina

ARTICLE INFO

Article history:
Received 26 May 2008
Received in revised form
22 August 2008
Available online 7 September 2008

Keywords:
Magnetic material
Magnetic susceptibility
Antiferromagnetism

ABSTRACT

Measurements of magnetic susceptibility χ, in the temperature range from 2 to 300 K, and of magnetization M vs. applied magnetic field B, up to 5 T, at various temperatures were made on polycrystalline samples of the Mn_2GeTe_4 compound. It was found that Mn_2GeTe_4 has a Néel temperature T_N of about 135 K, shows mainly antiferromagnetic behavior with a very weak superimposed ferromagnetic component that is attributed to spin canting. Also, the magnetic results suggest that a possible spin-glass transition takes place at $T_f \approx 45$ K. The spin-glass order parameter $q(T)$, determined from the susceptibility data, was found to be in agreement with the prediction of conventional spin-glass theory. The M vs. B results indicated that bound magnetic polarons (BMPs) occur in the compound, and that the effects from BMPs disappear at approximately 80 K. The M vs. B curves were well fitted by a Langevin type of equation, and the variation of the fitting parameters determined as a function of temperature. Using a simple spherical model, the radius of the BMP in the material was found to be about 27 Å; this value is similar to the effective Bohr radius for an acceptor in the II–IV–V_2 and I–III–VI_2 ternary semiconductor compounds.

1. Introduction

Magnetic semiconducting materials (MSMs) are of interest because of the manner in which the magnetic behavior associated with the concerned magnetic ion can modify and complement the semiconductor properties [1]. These MSMs have received attention because of their potential application in optoelectronic and magnetic devices. It has been found that the particular magnetic behavior occurring in any given case depends to a large extent on the distribution of the magnetic atoms in the lattice. Thus, for MSMs in which these atoms are at random in the cation lattice, the material mainly shows spin-glass form [1]. For MSMs, where the arrangement of magnetic atoms on the cation lattice is regular, a variety of magnetic states can occur, viz. antiferromagnetism, ferromagnetism, canted ferromagnetism, magnetic competition between magnetic neighbors leading to magnetic frustration, etc. [2,3]. Also, the presence of charge carries localized at the impurities can induce sizable magnetization in their vicinity or within the sphere of its effective Bohr orbit, i.e. formation of bound magnetic polarons (BMPs) [1], which affects the magnetic properties of the material such as the magnetization and susceptibility curves at low temperature, etc.

The materials that have been most studied are the semimagnetic semiconductor alloys obtained from the tetrahedrally coordinated II–VI semiconductor compounds by replacing a fraction of the group II cations with manganese, giving alloys such as $Cd_{1-z}Mn_zTe$ [1]. These studies have been extended to the investigation of the tetrahedrally coordinated I–III–VI_2, II–III_2–VI_4 and I_2–II–IV–VI_4 compounds and alloys [4–6]. Another group of semiconducting materials, which would show similar tetrahedrally bounded form, are the II_2–IV–VI_4 compounds. These materials can also be regarded as derived from the II–VI binaries, in which the cation has been substituted by two types of cations and an array of vacancies is introduced. The crystal structure of various II_2–IV–VI_4 compounds has been investigated by several workers [7], and it has been indicated that three structure types exit: a distorted spinel structure [8], an olivine-type structure (Mg_2SiO_4, space group Pnma, No. 62, $Z = 4$) and a structure type with the orthorhombic space group Cmmm reported for Mn_2SnS_4 [9].

Regarding the olivine structure of II_2–IV–VI_4, the anions are in almost regular hcp disposition, the IV cations are in tetrahedral coordination and the II cations are in distorted octahedral coordinations. In the case of the magnetic olivines (II = Mn, Fe and/or Co) there are four magnetic ions per cell on 4a sites with

* Corresponding author. Tel.: +58 274 2716979.
E-mail address: mquinter@ula.ve (M. Quintero).

0304-8853/$ - see front matter © 2008 Elsevier B.V. All rights reserved.
doi:10.1016/j.jmmm.2008.09.003

inversion symmetry and four on 4c sites with mirror symmetry, giving various magnetic configurations at low temperature. The magnetic properties of the Mn_2SiS_4 and Fe_2GeS_4 have been studied by magnetization and neutron diffraction measurements, and it was found that several different magnetic configurations in succession going from helium to room temperature occur in these compounds [10,11]. Neutron diffraction experiments, carried out on olivine samples of $Fe_{2-x}Zn_xSiO_4$, have revealed that, in addition to the above magnetic configurations, short-range magnetic order exists at low temperature [12]. The magnetic results obtained on amorphous samples of II_2SnTe_4 showed that these materials exhibit spin-glass behavior with an evident weak ferromagnetic component observed at low temperature [13]. However, as indicated by Mikus et al. [14], a comprehensive picture for the magnetic properties of this group of materials is still lacking.

In the present program of work, we are studying the properties of some II_2–IV–VI_4 materials with II = Mn, Fe; IV = Si, Ge, Sn and VI = Se, Te. The initial work on the crystallographic and magnetic properties of Mn_2GeTe_4, Fe_2GeTe_4 and Fe_2SnSe_4 compounds was already published in Ref. [15]. It was found that Mn_2GeTe_4 has an orthorhombic olivine-type structure with crystallographic parameter values of $a = 13.600(1)$ Å, $b = 10.745(1)$ Å, $c = 7.775(1)$ Å and $V = 1136.2(2)$ Å^3. The susceptibility curve for this material was shown but no detailed magnetic analysis was given. The aim of the present paper is to show some results on the magnetic properties of the Mn_2GeTe_4 compound.

2. Samples and measurements

The polycrystalline samples used were prepared by the usual melt and anneal technique. The appropriate amounts of the component elements were melted together, at 1150 °C for 3 h, and then cooled to 550 °C. After annealing at this temperature for 1 month, the ingot was very slowly cooled to room temperature. An X-ray powder diffraction pattern was recorded at 300 K to check the equilibrium conditions as well as the presence of secondary phases and to estimate lattice parameter values. Measurements of magnetic susceptibility χ as a function of temperature T in the range 2–300 K were made with a fixed value of magnetic field B of 100 G, using a Quantum Design SQUID magnetometer. Measurements of magnetization M as a function of applied field B up to 5 T were made at various fixed temperatures.

3. Results, analysis and discussions

The obtained magnetic susceptibility χ vs. temperature T curve for the Mn_2GeTe_4 is shown in Fig. 1 for $2\,K < T < 300\,K$, and the corresponding inverse of susceptibility $1/\chi$ vs. T curve is illustrated in Fig. 2. The resulting curves of magnetization M vs. applied magnetic field B obtained at various fixed temperatures are shown in Fig. 3. It is seen from Fig. 1 that in this range of T a transition occurs at about 45 K and below this temperature the susceptibility measurements carried out under zero-field cooling (ZFC) (heating run) and field cooling (FC) (cooling run) gave different results, i.e. temperature hysteresis is observed below $T_f \sim 45$ K. The difference in the two experiments is a common characteristic of magnetic disorder and frustration and could be a hallmark of a spin-glass state, in which the magnetic disorder is quenched and the interactions between spins are in conflict with each other leading to frustration. It is seen in Fig. 2 that another possible transition, which is clearly seen in the $d(1/\chi)/dT$ vs. T curve shown in the inset of Fig. 2, occurs at about 135 K, and, as will be suggested below, this one would involve a change from antiferromagnetic behavior between the localized Mn's spins to a paramagnetic state above 135 K. Also, it is found that, for data above 200 K, the reciprocal susceptibility seems to vary as $1/\chi \sim T - \theta_a$, with $\theta_a \sim -50$ K, giving an unexpected value of $\mu \sim 7.1\ \mu_B$,

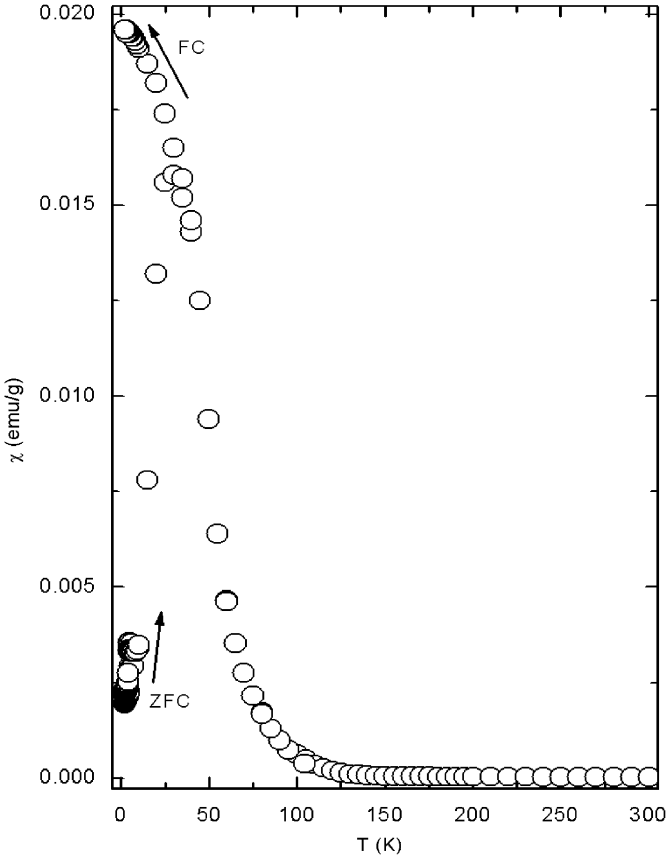

Fig. 1. Variation of magnetic susceptibility χ with T for the Mn_2GeTe_4 compound obtained with an applied field B of 100 G. The direction of the ZFC (heating run), or FC (cooling run), is indicated by the corresponding arrow.

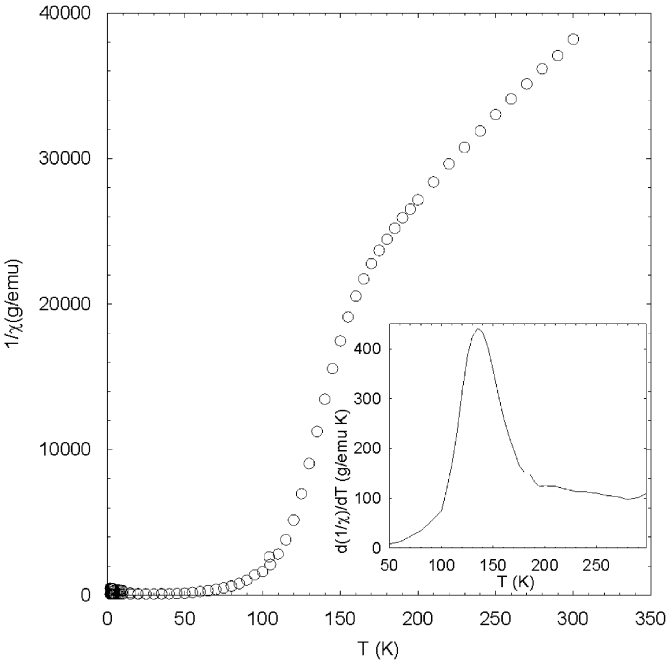

Fig. 2. Variation of $1/\chi$ with T for the Mn_2GeTe_4 compound. Inset: variation of $d(1/\chi)/dT$ with T.

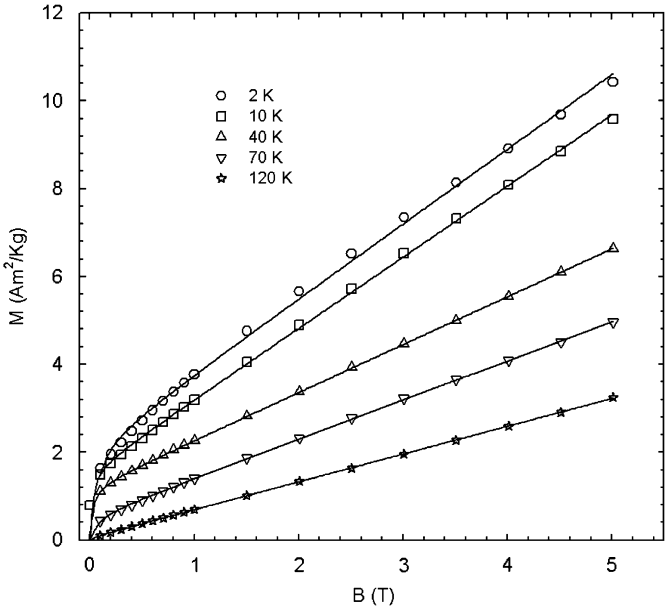

Fig. 3. Variation of magnetization M as a function of applied field B for a range of temperatures. Full lines: fits to Eq. (3). For the sake of clarity the curve at 4 K has been omitted.

which is higher than the expected value for the effective magnetic moment of Mn^{2+} ($S=\frac{5}{2}$ and $\mu_{eff}=5.92\,\mu_B$). It is to be mentioned that, with the present results, the reliability and/or an explanation on this point could not be given here; in order to obtain clearer information on the overall form of the $1/\chi$ vs. T curve, and hence to understand more on this behavior, it is necessary to carry out experimental work above 300 K, the upper temperature limit of the present measurements. Nevertheless, it is to be noted that the curve in Fig. 2 seems to have a form that is similar to that of a ferrimagnetic material with Néel temperature $T_N=135$ K. Thus, when the Néel theory of ferrimagnetism [16], $C/\chi=T-\theta_a-(T_N-\theta_a)(T_N-\theta)/(T-\theta)$, was used to fit the experimental curve in Fig. 2, it was found that not good fit to the $1/\chi$ vs. T data could be obtained. This result, together with the M vs. B data to be discussed below, would suggest that below T_N the Mn_2GeTe_4 is not ferrimagnetic and, as was indicated above, instead it consists of antiferromagnetically couple planes of spins with a possible very weak superimposed ferromagnetic component that could be attributed to spin canting, and this mechanism can give similar $1/\chi$ vs. T curve. This magnetic configuration has been observed by Bodenan et al. [17] in samples of olivine Mn_2SiSe_4. It is to be mentioned that no spontaneous magnetic moment, usually shown by ferrimagnetics, as well as no evident magnetic hysteresis were observed in the magnetization M vs. applied magnetic field B data obtained at each temperature investigated; this would indicate that the canted component is very small and that the transition at 135 K is from an antiferromagnetic to a paramagnetic state. This transition will be further discussed below. As was indicated by Mikus et al. [14], the explanation for the very weak ferromagnetic component that was derived from earlier magnetic susceptibility measurements [14,17] remains still speculative, and it may result from local non-zero components that do not show up in the overall magnetic structure. The M vs. B results will be discussed further below.

Returning to the χ vs. T and $1/\chi$ vs. T curves of Figs. 1 and 2, respectively, the observed temperature hysteresis below $T_f=45$ K, and the change of slope around 135 K, together with the absence of magnetic hysteresis as well as spontaneous magnetic moment in the M vs. B results would suggest that, again, a transition involving a change from long-range antiferromagnetic behavior, between the localized Mn's spins, to a paramagnetic state occurs at the Néel temperature $T_N\approx135$ K, with a possible spin-glass transition at about 45 K. Similar magnetic frustration has been reported by Holger et al. [14] in amorphous samples of Co_2SnTe_4 and by Haushalter et al. [18] in samples of M_2SnTe_4 with M = Cr, Mn, Fe, Co. Short-range magnetic order has been observed in samples of $Fe_{2-x}Zn_xSiO_4$ [12]. To describe the spin-glass state theoretically, Edwards and Anderson introduced a spin-glass order parameter q as a function of temperature T [19]. Based on the appropriate form of the mean-field theory (MFT), Sherrington and Kirkpatrick predicted that the spin-glass order parameter $q(T)$ vanishes at the freezing temperature T_f and it is proportional to $(1-T/T_f)$ below T_f [20,21]. The value of $q(T)$ can be extracted from the magnetic susceptibility, but treating C and θ as effective spin-glass parameters rather than the true constants, i.e. the effective spin-glass Curie constant C_{SG}, and the effective spin-glass Curie–Weiss temperature θ_{SG}, as follows [22]:

$$q(T)=1-\frac{T\chi(T)}{C_{SG}+\theta_{SG}\chi(T)} \tag{1}$$

An effective spin-glass Curie constant ($C_{SG}=44.4$ emu K/mol Oe) and an effective spin-glass Curie–Weiss temperature ($\theta_{SG}=45$ K) are obtained by fitting the susceptibility with the Curie–Weiss-like law from 55 to about 75 K (Fig. 4). Fig. 5 displays the temperature dependence of the spin-glass order parameter $q(T)$. It is seen that the value of $q(T)$ drops to zero at $T_f\approx45$ K as was mentioned above. In the inset of Fig. 5, the normalized order parameter $q(T/T_f)$ is plotted vs. the normalized temperature $(T_f-T)/T_f$ together with the resulting data fitted by the equation:

$$q(T/T_f)=q_0(T/T_f)+a((T-T_f)/T_f)^b \tag{2}$$

From the fit it was obtained $q_0=0.033\pm0.0001$, $a=0.97\pm0.001$ and $b=1.08\pm0.003$, close to the values predicted by the MFT [20].

Turning to the M vs. B curves for Mn_2GeTe_4, it can be seen that the data in Fig. 3 showed the general form expected when BMPs

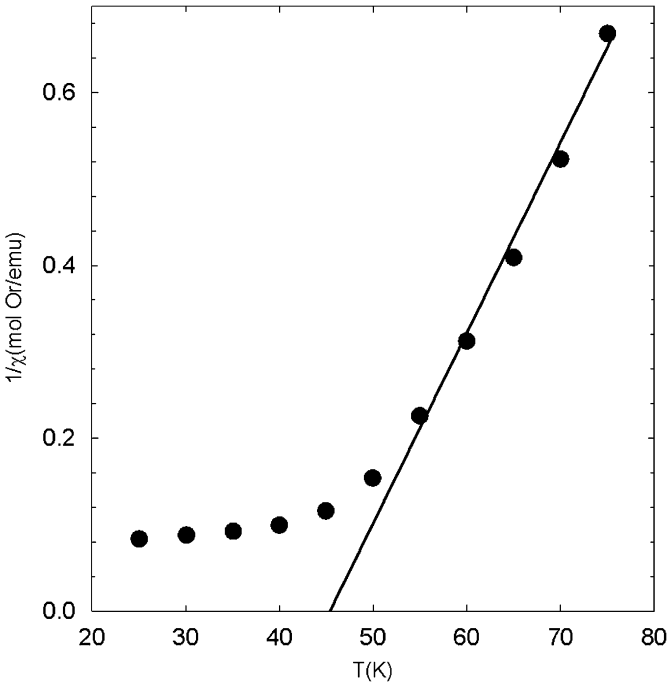

Fig. 4. Variation of $1/\chi(T)$ between 20 and 80 K. The solid line is a linear regression extrapolated to the temperature axis.

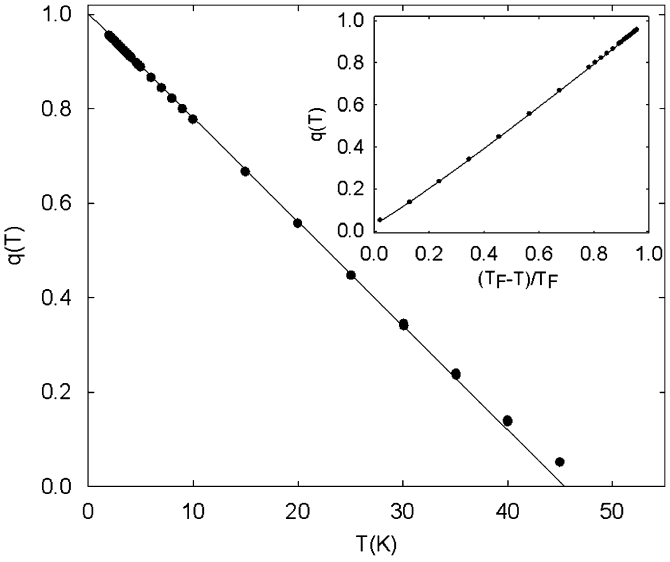

Fig. 5. Variation of the order parameter q as a function of temperature T, the solid line indicates the mean field theory prediction. Inset: variation of the normalized order parameter $q(T/T_f)$ vs. $(T_f-T)/T_f$; the line represents the fit to Eq. (2).

are present in the material. In this figure it is seen that the spacing and shape of the curves are of the same regular form given previously [23,24] for other materials showing BMP effects. From the form of the M vs. B curves, it is seen that, within the limits of experimental errors, the magnitude of the BMPs resultant moment falls with increasing temperature, becoming practically zero at about 120 K, where the linear form of the graph corresponds to antiferromagnetic behavior. These results suggest that the present magnetization data could be analyzed in terms of BMPs. Thus, the M vs. B curves for BMPs can be very well fitted to an equation of the form:

$$M = M_0 L(x) + \chi_m B \tag{3}$$

where the Langevin term $L(x)$ $(=\coth x - 1/x)$ represents the contribution of BMPs and the term $\chi_m B$ the contribution of the matrix. Here, $M_0 = Nm_s$ and $x = m_{eff}\, B/K_B T$ where N is the number of BMPs involved, m_s and m_{eff} are, respectively, the true and effective spontaneous moments per BMP. In the Langevin function, the effective moment m_{eff} determines how quickly the true moment aligns along B. Because of the effects of interaction between the BMPs, it was proposed that $m_{eff} \approx m_s T/(T+T')$, where T' represents the interaction [23]. With T' relatively small, at the higher temperatures investigated, to a good approximation $m_{eff} \approx m_s$. Thus, for a good approximation, the M vs. B data can be analyzed in terms of Eq. (1), with M_0, m_{eff} and χ_m used as fitting parameters. The resulting fitted curves are shown in Fig. 3, where it is seen that in each case, a good fit was obtained. Values of the fitting parameters were thus determined as a function of temperature, and these are plotted against T in Fig. 6.

At higher temperatures, in the range where $m_{eff} \approx m_s$, values for N can be obtained from the ratio M_0/m_{eff}. In Fig. 7a, values are shown for M_0/m_{eff} $(=N)$ as a function of T. It is seen that, within the limits of experimental errors, in the range $15\,K \leqslant T \leqslant 80\,K$, the value of N tends to level out and is almost constant with a mean value of $5.01 \times 10^{-4}\,Am^2/Kg\,\mu_B$, this is illustrated in the inset of Fig. 7a. This mean value of N gives a concentration of non-ionized acceptors of $5.5 \times 10^{16}/cm^3$. Using this value for N, values for m_s can be obtained from the M_0 values and the resultant variation of m_s with T is shown in Fig. 7b. It is seen that, within the limits

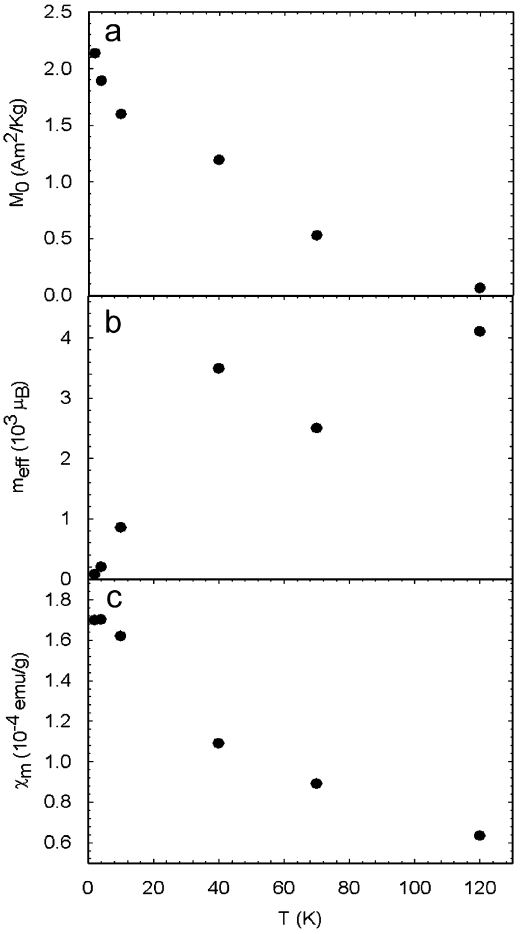

Fig. 6. Mn_2GeTe_4: (a) total BMP magnetization M_0 $(=Nm_s)$ vs. T, (b) effective moment per BMP m_{eff} vs. T and (c) susceptibility χ_m vs. T.

of experimental errors, and in the range where N is nearly independent of T, the variation of m_s with T is practically linear, and extrapolates to a value of about $3400\,\mu_B$/BMP at $T = 0$ K. Taking the magnetic moment for Mn^{2+} as $5.9\,\mu_B$ gives the mean number of Mn atoms in each BMP as 566. The assumption that in a very simple model all Mn ions inside a spherical BMP are aligned and that none outside the sphere contribute gives the radius of the BMP to be 27 Å. This value is higher than the typical effective Bohr radius for an acceptor in the II–VI materials. However, using the standard values of $\varepsilon_o \approx 12$ for the static dielectric constant and $m_h \approx 0.25 m_o$ for the hole effective mass, a typical value of 25 Å is obtained for the effective Bohr radius for an acceptor in the II–IV–V_2 and I–III–VI_2 semiconductor compounds [25], which is close to the value obtained here.

4. Conclusions

The magnetic results suggest that, at about $T_N \approx 135$ K, the Mn_2GeTe_4 compound consists of antiferromagnetically couple planes of spins with a very weak superimposed canted ferromagnetic component; similar magnetic configurations have been reported earlier for this type of material. The observed temperature hysteresis in the susceptibility curve together with the M vs. B results suggest that a spin-glass transition occurs at about 45 K. The variation of the order parameter $q(T)$ was found to be typical of a spin-glass state, giving parameter values in good agreement with the prediction of the MFT.

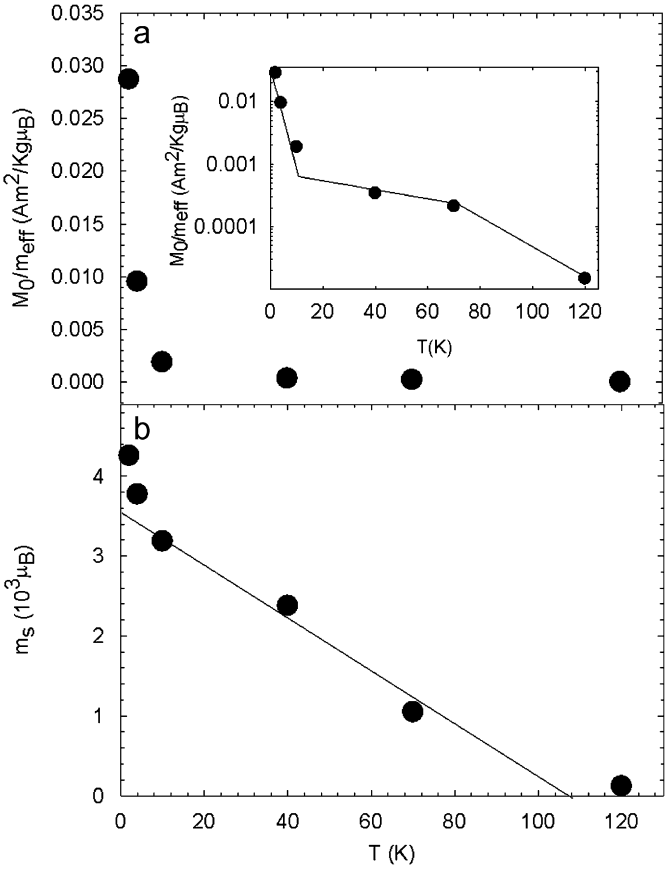

Fig. 7. Variation with T of (a) the numbers of BMPs N, (b) the spontaneous moment of a BMP m_s.

From the measurements of M vs. B, it is seen that BMPs occur below ~80 K. Analysis of the M vs. B curves by fitting to a Langevin type of equation gave values for the number of BMPs, the average magnetic moment and hence the average size of a BMP. These values were found to be consistent with previously published data.

Acknowledgements

This work was supported by the CDCHT-ULA (Projects no. C-1436-06-05-AA, C-1437-06-05-Ed, C-1438-06-05-F, C-1532-07-05-B and C-1547-08-05-B) (Mérida-Venezuela) and FONACIT (Project no. LAB-97000821).

References

[1] J.K. Furdyna, J. Kossut, in: R.K. Willardson, A.C. Beer (Eds.), Diluted Magnetic Semiconductors, Semiconductors and Semimetals, vol. 25, Academic Press, New York, 1988.
[2] V. Baron, O. Amcoff, T. Ericsson, J. Magn. Magn. Mater. 195 (1999) 81.
[3] D. Chowdhury, Spin Glasses and Other Frustrated Systems, Princeton Series in Physics, Princeton University Press, World Scientific Publishing Co Pte Ltd., New Jersey, 1986.
[4] M. Quintero, M. Lopez, M. Morocoima, A. Rivero, P. Bocaranda, J.C. Woolley, Phys. Status Solidi (b) 193 (1996) 325.
[5] M. Morocoima, M. Quintero, E. Quintero, P. Bocaranda, J. Ruiz, E. Moreno, J. Appl. Phys. 100 (2006) 073902.
[6] E. Quintero, M. Quintero, E. Moreno, M. Morocoima, P. Grima, P. Bocaranda, J.A. Henao, J. Pinilla, J. Alloys Compds. (2008).
[7] J.A. Henao, J.M. Delgado, M. Quintero, Powder Diffr. 12 (2) (1997) 1.
[8] J.C. Jumas, E. Philippot, M. Maurin, Acta Crystallogr. Sect. B 33 (1977) 3850.
[9] M. Wintenberger, J.C. Jumas, Acta Crystallogr. Sect. B 36 (1980) 1993.
[10] H. Vincent, E.F. Bertaut, J. Phys. Chem. Solids 34 (1973) 151.
[11] A. Junod, K.-Q. Wang, G. Triscone, G. Lamarche, J. Magn. Magn. Mater. 146 (1995) 21.
[12] M.K. Krause, R. Sonntag, C.A. Kleint, E. Ronsch, N. Stusser, Physica B 213 and 214 (1995) 230.
[13] J.W. Foise, C.J. O'Connor, R.C. Haushalter, Solid State Commun. 63 (4) (1987) 349.
[14] Holger Mikus, Hans-Jörg Deiseroth, Krassimir Aleksandrov, Clemens Ritter, Reinhard K. Kremer, Eur. J. Inorg. Chem. (2007) 1515.
[15] M. Quintero, D. Ferrer, D. Caldera, E. Moreno, E. Quintero, M. Morocoima, P. Grima, P. Bocaranda, G.E. Delgado, J.A. Henao, J. Alloys Compds. (2008).
[16] J.S. Smart, Effective Field Theories of Magnetism, W.B. Saunders Company, Philadelphia and London, 1966, p. 113.
[17] F. Bodenan, V.B. Cajipe, G. Ouvrard, G. Andre, J. Magn. Magn. Mater. 164 (1996) 233.
[18] R.C. Haushalter, C.J. O'Connor, A.M. Umarji, Solid State Commun. 49 (10) (1984) 929.
[19] S.F. Edwards, P.W. Anderson, J. Phys. F: Met. Phys. 5 (1975) 965.
[20] D. Sherrington, S. Kirkpatrick, Phys. Rev. Lett. 35 (1975) 1972.
[21] S. Kirkpatrick, D. Sherrington, Phys. Rev. B 17 (1978) 4384.
[22] T. Mizoguchi, T.R. McGuire, S. Kirkpatrick, J.R. Gambino, Phys. Rev. Lett. 38 (1977) 89.
[23] G.H. McCabe, T. Fries, M.T. Liu, Y. Shapira, L.R. Ram-Mohan, R. Kershaw, A. Wold, C. Fau, M. Averous, E.J. McNiff Jr., Phys. Rev. B 56 (1997) 673.
[24] E. Quintero, M. Quintero, M. Morocoima, P. Bocaranda, J. Appl. Phys. 102 (8) (2007) 083905.
[25] J.L. Shay, J.H. Wernick, Ternary Chalcopyrite Semiconductors, Pergamon, Oxford, 1975.